Fernández-Ruiz, M.R., Martins, H. F., Pastor-Graells, J., Martin-Lopez, S., Gonzalez-Herraez, M., 2016, "Phase-sensitive OTDR probe pulse shapes robust against modulation-instability fading," Optics Letters, 41, n. 24, pp. 5756-5759.

Available at http://dx.doi.org/10.1364/OL.41.005756

Phase-sensitive OTDR probe pulse shapes robust against modulation-instability fading

María R. Fernández-Ruiz,[1,*] Hugo F. Martins,[2] Juan Pastor-Graells,[1] Sonia Martin-Lopez,[1] and Miguel Gonzalez-Herraez[1]

[1]Departamento de Electrónica, Universidad de Alcalá, Escuela Politécnica Superior, 28871, Madrid, Spain
[2]FOCUS S.L., C/ Orellana, 1, 1º Izquierda, 28804, Madrid, Spain
*Corresponding author: rosario.fernandez@uah.es

Received XX Month XXXX; revised XX Month, XXXX; accepted XX Month XXXX; posted XX Month XXXX (Doc. ID XXXXX); published XX Month XXXX

Typical phase-sensitive optical-time domain reflectometry (φOTDR) schemes rely on the use of coherent rectangular-shaped probe pulses. In these systems, there is a trade-off between the signal-to-noise ratio (SNR), spatial resolution and operating range of the φOTDR system. To increase any of these parameters, an increase in the pulse peak power is usually indispensable. However, as it is well-known, there is a limit in the allowable increase in probe power due to the onset of undesired nonlinear effects such as modulation instability. In this Letter, we perform an analysis of the effect of the probe pulse shape on the visibility fading due to modulation instability. In particular, four different temporal profiles are chosen, namely, rectangular, Gaussian, triangular and super-Gaussian (order 2). Our numerical and experimental analyses reveal that the use of triangular or Gaussian-like pulses can significantly inhibit the visibility fading issues. As such, an increase in the range up to two-fold for the same pulse energy (i.e., SNR) and nominal spatial resolution can be achieved, as compared with the results obtained when using rectangular pulses. This is due to a more robust behavior of the Gaussian and triangular pulses against the Fermi-Pasta-Ulam (FPU) recurrence occurring in modulation instability.

OCIS codes: *(060.2370) Fiber optics sensors; (120.4825) Optical time domain reflectometry; (290.5870) Scattering, Rayleigh; (320.5540) Pulse shaping; (190.4370) Nonlinear optics, fibers.*

http://dx.doi.org/10.1364/OL.99.099999

Distributed optical fiber sensing using Rayleigh-based phase sensitive optical time-domain reflectometry (φOTDR) is gaining a great deal of interest in areas such as structure health monitoring, aerospace or material processing [1,2]. φOTDR-based sensors are routinely employed for the monitoring of mechanical variations (e.g., vibrations, displacements, etc.) over large perimeters. Recent advances have demonstrated the capability of φOTDR sensors for measuring temperature and strain changes in a simple and elegant fashion [3], increasing the accuracy and reducing the measurement time in two orders of magnitude with respect to that of typically-used Brillouin scattering-based sensors [4]. This fact, together with their potential for higher spatial resolution and bandwidth than other available distributed sensors make φOTDR an interesting technology solution for a wide number of applications.

In φOTDR-based sensing schemes, a highly coherent optical pulse is injected into the sensing fiber. The received power trace is produced by coherent interference of the light reflected via Rayleigh scattering in the inhomogeneities of the fiber. This yields in traces that show a static, noise-like interference pattern. Ideally, the probe pulse should be as narrow as possible to achieve high spatial resolution measurements, and it should have as much energy as possible to achieve the best possible signal-to-noise ratio (SNR) in detection. This combination leads to high peak power pulses, which are subject to nonlinear impairments in their propagation along the sensing fiber, that degrade the received backscatter trace as well as the effective sensing detection [5]. Preventing these effects imposes a maximum peak power of optical pulses, which in turn limits the SNR (and hence the measurement range) of the received backscatter trace. To improve these parameters, it is necessary to broaden the probe pulse width, which, at the same time, deteriorates the spatial resolution of the system. Hence, there is a trade-off between the spatial resolution (pulse width), length range (pulse peak power) and SNR of the received power trace.

To date, the use of rectangular-like pulses is the norm in φOTDR schemes. Most of the φOTDR sensing systems employ rectangular-like probe pulses with widths of tens or hundreds of nanoseconds and peak powers under 1 W, which provide power traces of several kilometers with acceptable SNR. In the literature, the effect of the probe pulse shape in the sensor performance has been investigated in the case of Brillouin-based distributed sensors [6]. This study has determined that the use of rectangular pulses is more convenient than other narrower-bandwidth shapes (e.g., Gaussian-like) for Brillouin sensors, since rectangular-shaped pulses suffer less spectral broadening due to self-phase modulation (SPM), leading to

a better determination of the Brillouin gain spectrum along the fiber. However, a similar analysis has not been done for φOTDR technology to date. Considering that the principle of operation of φOTDR systems is substantially different from that of Brillouin-based sensors, it is interesting to investigate the optimal pulse shape specifically for this type of sensors. Indeed, the most important consideration in this type of sensors is not so much the spectral content of the pulse, but rather the visibility of the trace along the fiber. Rectangular-shaped pulses show a continuous level of light power along a relatively long temporal width, which induces a reversible power exchange between the probe and the sidebands amplified by the modulation instability gain at well-defined peak frequencies. This effect is known as the Fermi-Pasta-Ulam (FPU) recurrence, and it is ultimately responsible of a significant reduction of the trace visibility at specific positions in the trace [5,7].

In this Letter, we present an analysis of the impact of the probe pulse shape in the backscatter trace of φOTDR-based sensing systems. In particular, we compare the traces received after launching probe pulses into the fiber with the same energy and nominal spatial resolution (defined considering the full-width at half maximum (FWHM) of the probe pulses) and four different shapes, namely, Gaussian-like, triangular, super-Gaussian (order 2) and rectangular. We perform numerical simulations that are subsequently validated by an experimental demonstration. Our analysis shows that the use of rectangular-like pulses is the most detrimental for sustaining an adequate visibility (and consequently, sensing sensitivity) all along the received power trace. Gaussian and triangular-shaped pulses show a better behavior in terms of evolution of the visibility along the distance, which should reflect into a better sensing performance.

Prior to the realization of experimental tests, we have carried out a series of numerical simulations that have helped us to identify notable differences in the obtained power trace depending on the shape of the probe pulse envelope. The algorithm employed in the numerical simulations has been developed as follows: first, the propagation of the probe pulse is simulated by solving the nonlinear Schrödinger equation (NLSE) using a Split-Step Fourier Method with adaptive step size [8].

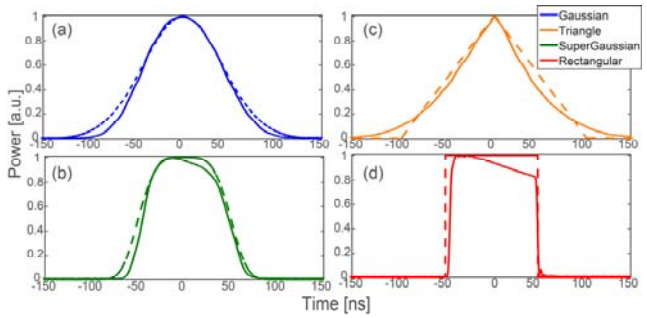

Fig. 1. Input pulses launched into the φOTDR system. Dashed lines represent the pulses employed in numerical simulations, while solid lines show the pulses employed in the experimental demonstration.

Figure 1 shows the input pulse shapes employed in the numerical simulations (in dashed line), and compares them with the modulated probe pulses subsequently employed in the experimental demonstrations (in solid line). All the pulses are centered at 1550 nm, and all of them have a FWHM of 100 ns (i.e. all of them achieve the same nominal spatial resolution). Two different values of pulse energy have been employed, namely, 91 nJ and 165 nJ. The peak power of the different pulses has been adapted to achieve the aforementioned pulse energy, with the aim of generating traces that maintain the same SNR. The corresponding values of peak power are 910 mW and 1650 mW, respectively, in the case of rectangular pulses. For the simulations, the sensing fiber is considered to be a 25 km- long single-mode fiber (SMF-28). The specifications of the fiber are: nonlinear coefficient $\gamma = 1.1\ W^{-1}\ km^{-1}$, second order dispersion parameter $\beta_2 = -21.7\ ps^2/km$, and attenuation $\alpha = 0.2$ dB/km.

Once the evolution of the optical pulse is known, the Rayleigh scattering process is simulated using the algorithm described in Ref. [9]. In particular, the backscattering process is modelled by a set of discrete scatterers (reflectors) whose amplitude and phase are characterized as statistically independent random Gaussian variables, while their coordinates are deterministic (the random phase of the scatterers contributes to the final backscatter trace as if they had randomly distributed positions). The complex envelope of the optical probe pulse is updated while it propagates along the fiber, employing the results obtained from the NLSE resolution. Finally, the power trace is calculated from the resulting backscattered electromagnetic field by modeling the effect of a photodetector: the back-reflected optical intensity is computed as a function of the time of flight of the pulse in the fiber, and the resulting signal is low-pass filtered according to the detection bandwidth of the photodetector. In this case, the bandwidth of the considered photodetector is 125 MHz. The visibility of the resulting traces is plotted in Fig. 2, which is computed as [5]:

$$V = (T_{\max} - T_{\min}) / (T_{\max} + T_{\min}), \qquad (1)$$

where $T_{\max}$ and $T_{\min}$ are the maximum and minimum values of the trace over a certain distance record. In order to obtain a good estimation of the trace visibility, the size of the employed window should contain a statistically relevant number of trace maxima and minima. Generally, a window of several times the spatial resolution of the trace (~10 m in this case) is considered. In this case, a window of 60 m has been employed.

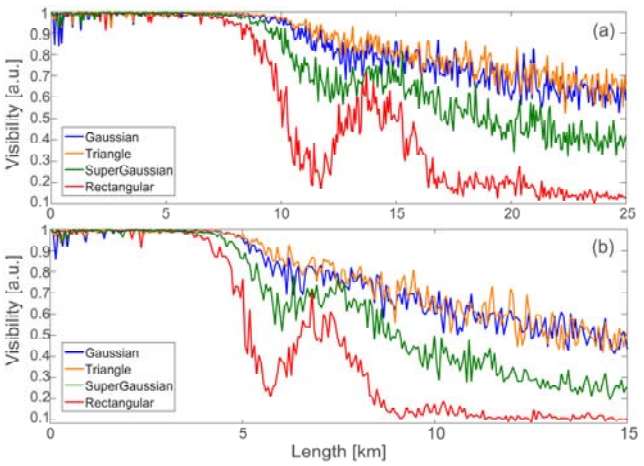

Fig. 2. Visibility of the numerically obtained power trace. (a) Visibility obtained when the energy of the input pulses is 91 nJ; (b) Visibility for an input pulse energy of 165 nJ.

Note that in the case of propagation of pulses with 165 nJ of energy, only a 15 km-long trace is presented, since no additional information can be extracted from the last 10 km of trace. From the obtained numerical results, we observe that if rectangular pulses are used as probe, the power trace suffers from fading at certain specific positions along the trace. At those positions, the sensing sensitivity is nearly lost. The positions where fading occurs are closer to the input end of the fiber for higher values of peak power, leading to a shorter usable length range of the sensors. However, when using probe pulses whose power is not constant along its width, e.g., with Gaussian-like or triangular shapes, the modulation instability-induced trace fading is significantly reduced. The reason is to be found in the different behavior of the FPU recurrence associated to modulation instability with these probe pulse shapes.

Modulation instability manifests as a breakup of continuous wave (CW) or quasi-CW radiation into a train optical pulses [10]. The propagation of (quasi-) CW light is inherently unstable under anomalous dispersion. As a result, the signal of interest acts as a pump in an amplification process of any small perturbation (e.g., noise) present into the gain spectrum of modulation instability, leading to a depletion of the signal power. In Fig. 2, we observe that the visibility of all the traces decreases starting from a certain fiber length, namely ~10 km for pulses with energy of 91 nJ and ~5 km for pulses of 165 nJ, due to modulation instability. However, in the case of rectangular or super-Gaussian pulses, the trace visibility presents a strong fading immediately after those locations, and it is subsequently partially recovered, forming several lobes. Those lobes that appear in the visibility trace are caused by the FPU recurrence phenomenon [5]: the quasi-CW radiation (rectangular pulses) fosters an oscillating energy transfer between the initial pulsed light and the high-order amplified beams. FPU recurrence requires a precise balance of energy transfer between a significant number of spectral modes. This situation is not accomplished when the pulse shape does not maintain the power level over a certain temporal width (i.e., when the pulse is not rectangular). In those cases, the different intensity levels are associated with different modulation instability gains and frequencies, destroying the FPU process [7]. As we may observe, the trace obtained from a triangular or Gaussian input pulse barely suffers from FPU recurrence and the trace visibility decreases in a smoother fashion than that obtained from rectangular pulses. The behavioral pattern observed from the simulation results states that the further is the pulse envelope shape from rectangular, the smoother is the reduction of visibility due to FPU recurrence of the modulation unstable probe pulses for the same energy and same FWHM. We have verified through simulations that the effect of SPM of the pulses, contrary to the case of Brillouin-based sensors [6], barely affects the final power trace as long as the spectral broadening of the pulse lies within the photodetector bandwidth. Otherwise, the smooth visibility decay of the traces will have an additional, reduced component due to the power filtered out by the photodetector.

The presented numerical results have been validated through an experimental demonstration. The setup employed is depicted in Fig. 3. There, an external cavity laser (ECL) laser generates the CW light at a wavelength of 1550 nm. Then, the target power envelope, which is electrically generated using a signal generator (SG), is carved in the CW light using a semiconductor optical amplifier (SOA). The pulse is amplified using an Erbium-doped fiber amplifier (EDFA) up to have the same peak power of the pulses employed in the numerical analysis. The synthesized shape and power of the pulses are verified using a control arm located after the EDFA (the measurements at this point are shown if Fig. 1, in solid line). The slope in the peak power of the generated pulses, clearly observed in the super-Gaussian and rectangular-like shapes, is due to the non-constant amplification gain of the SOA. A dense wavelength division multiplexer (DWDM) is employed to filter out the amplified spontaneous emission (ASE) noise from the EDFA, and the resulting pulses propagate through a single mode fiber of 25 km. The received amplified traces are detected using a 125 MHz-bandwidth photodetector, and are plotted in Fig. 4.

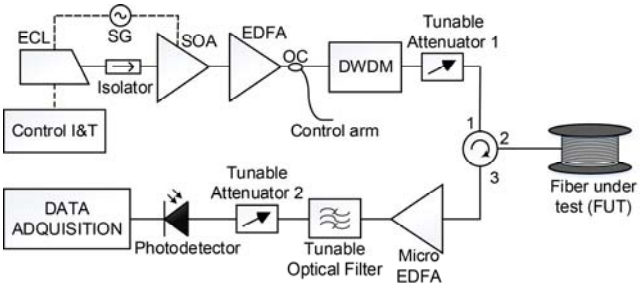

Fig. 3. Experimental setup. ECL: External cavity laser; SG: Signal generator; SOA: Semiconductor optical amplifier; EDFA: Erbium-doped fiber amplifier; OC: Optical coupler; DWDM: Dense wavelength division multiplexer; I&T, intensity & temperature.

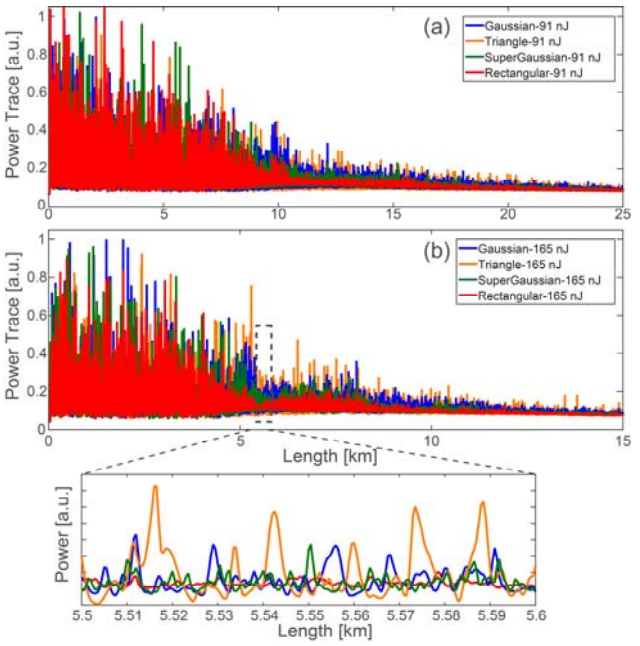

Fig. 4. Experimental backscatter power trace from the different realizations of the experiment. (a) Power traces obtained when the energy of input pulses is 91 nJ; (b) Power traces for input pulse's energy of 165 nJ.

Figure 4(a) compares the measured power traces for different input pulse shapes and a pulse energy of 91 nJ. For this value of peak power and rectangular pulses, the first fading induced by FPU recurrence occurs at around 11 km. Figure 4(b) shows a similar comparison, but in this case the input pulse energy is 165 nJ. For this value of energy, the fading induced by FPU recurrence is more pronounced, and with rectangular pulses, the first fading point occurs at about 5.5 km.

These experimental results are in line with the previously presented simulations results. Note that at fading points, the trace practically disappears when rectangular pulses are employed (see the zoomed trace in Fig. 4(c)). However, the fading is highly reduced for different pulse shapes. For example, when a probe pulse with Gaussian or triangular-like power envelope (blue and yellow line, respectively) is employed, there is a certain visibility loss at the specified lengths (i.e., 11 km for a pulse energy of 91 nJ and 5.5 km for energy of 165 nJ), but the trace is still visible at those points. As such, by varying the power shape of the probe pulse, it is possible to increase the length range of φOTDR-based sensor systems while keeping the sensor resolution. The visibility of the measured traces is calculated using Eq. 1. A window of 60 m has been employed for obtaining the maximum and minimum values of the power trace, similarly to the numerical analysis. The obtained visibility curves are plotted in Fig. 5.

We observe that the evolution of the trace visibility is very similar in our numerical and experimental results. In both situations, the graphs show the same pattern in terms of visibility vs. probe pulse shape. The differences between these results are associated to an imperfect matching between the experimentally achieved peak powers as compared with the numerical ones. Moreover, it is worth noting that in the simulations, the effect of polarization has been neglected, and as such, a unidimensional problem is considered. In practice, the sum of the two orthogonal polarizations reduces the visibility of the final trace [11]. Moreover, the experimentally obtained traces have been averaged to reduce the noise.

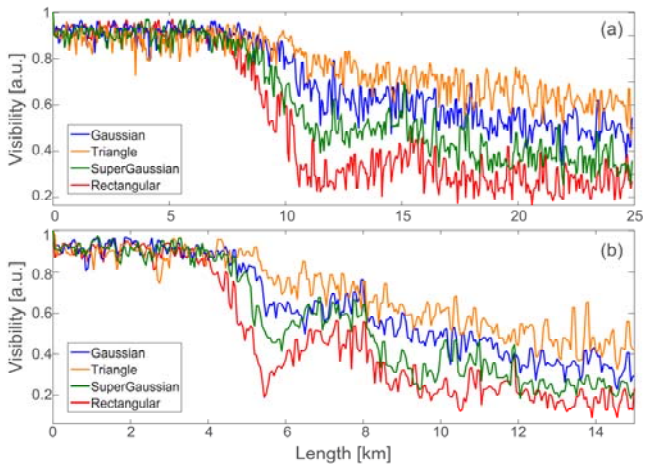

Fig. 5. Visibility of the experimentally measured power trace. (a) Visibility obtained when the energy of the input pulses is 91 nJ; (b) Visibility for input pulse's energy of 165 nJ.

The averaged traces have a sufficiently high SNR so that the effect of noise on the calculated visibility can be neglected. Indeed, the phase noise, together with temperature drifts occurred during the averaging process may also contribute to the fact that the visibility obtained from the experimental results is lower than the numerically obtained visibility. It should be noted that changing the pulse width slightly has no effect on the conclusions of this study.

In conclusion, in this Letter we have analyzed the impact of the use of probe pulses with different beamshapes on the backscatter power trace of φOTDR systems. The obtained results indicate that the typically used rectangular-like pulses are the most detrimental for the length range and sensitivity of φOTDR-based sensors, while the use of Gaussian or triangular-like pulses contributes to a smoother reduction of trace's visibility along the sensing fiber length. A Gaussian or triangular envelope pulse limits the effect of modulation instability and mitigates the advent of FPU recurrence, which enables an increase of the length range and sensitivity of the sensing system for the same peak power and nominal spatial resolution. The experimental validation of our analysis suggests that under comparable conditions, (same peak power and same nominal spatial resolution), the length range of the sensor can be duplicated by using a Gaussian-envelope pulse instead of a rectangular one.

Acknowledgment. This work was supported in part by: the European Research Council through project U FINE (Grant 307441); the European Commission through project MSCA-ITN-ETN-722509; the DOMINO Water JPI project, under the WaterWorks2014 cofounded call by EC Horizon 2020 and Spanish MINECO; the Spanish MINECO through projects TEC2013-45265-R and TEC2015-71127-C2-2-R; and the regional program SINFOTON-CM: S2013/MIT-2790. The work of Hugo F. Martins was supported by EU funding through the FP7 ITN ICONE program, gr. #608099. The work of Juan Pastor-Graells and Sonia Martín-López was supported by the Spanish MINECO through FPI and "Ramón y Cajal" Contracts, respectively.

References

1. J. M López-Higuera, L. Rodríguez Cobo, A. Quintela Incera, and A. Cobo, J. Lightw. Technol. 2**9,** 587 (2011).
2. A. Barrias, J. R. Casas, and S. Villalba, Sensors **16**, 748 (2016).
3. J. Pastor-Graells, H. F. Martins, A. García-Ruiz, S. Martín-López, and M. González-Herráez, Opt. Express 24, 13121 (2016).
4. A. Motil, A. Bergman, and M. Tur, Opt. Laser Technol. 78, 81 (2016).
5. H. F. Martins, S. Martín-López, P. Corredera, P. Salgado, O. Frazão, and M. González-Herráez, Opt. Lett. **38**, 872 (2013).
6. S. M. Foaleng, F. Rodríguez-Barrios, S. Martín-López, M. González-Herráez, and Luc Thévenaz, Opt. Lett. **36**, 97 (2011).
7. G. Van Simaeys, Ph. Emplit, and M. Haelterman, Phys. Review Lett. 87, 033902 (2001).
8. O. V. Sinkin, R. Holzlöhner, John Zweck, and C. R. Menyuk, J. Lightw. Technol. **21**, 61 (2003).
9. L. B. Liokumovich, N. A. Ushakov, O. I. Kotov, M. A. Bisyarin, and A. H. Hartog, J. Lightw. Technol. **33**, 3660 (2015).
10. G. P. Agrawal, *Nonlinear Fiber Optics*, 3rd ed. (Academic, 2001).
11. H. F. Martins, K. Shi, B. C. Thomsen, S. Martín-López, M. González-Herráez, and S. J. Savory, Opt. Express **24**, 22303 (2016).